An Automatic Coarse-Graining and Fine-Graining Simulation Method: Application on Polyethylene

Li-Jun Chen, Hu-Jun Qian, Zhong-Yuan Lu,* Ze-Sheng Li, and Chia-Chung Sun

State Key Laboratory of Theoretical and Computational Chemistry, Institute of Theoretical Chemistry, Jilin University, Changchun 130023, China

Multiscale modeling of a polymeric system is a challenging task in polymer physics. Here we introduce a bottom-up and then top-down scheme for the simulation of polyethylene (PE). The coarse-grained numerical potential for PE is derived through an automatic updating program by mapping its radial distribution function (RDF) from the Lowe–Andersen temperature controlling (LA) simulation onto the one from detailed molecular dynamics (MD) simulation. This coarse-grained numerical potential can be applied in larger systems under the same thermodynamic conditions. We have tested the reliability of the derived potential in two ways. First, the blends of different linear low-density polyethylene (LLDPE) with high-density polyethylene (HDPE) have been simulated in LA with the coarse-grained numerical potentials and reasonable results are obtained. Moreover, Rouse scaling behavior is reproduced for monodispersed polymeric systems with different chain lengths. The atomistic details of the beads can be reintroduced into the coarse-grained HDPE and LLDPE/HDPE models, followed by a few MD runs to alleviate the local tension induced by this fine-graining procedure. The equilibrated large atomistic system can then be used for further studies.

1. Introduction

Because of the long chain characteristics of polymers, the physical properties are multiscaled on both the length and the time scales. For example, it ranges from 10^{-10} m for the size of the backbone bond to 10^{-8} m for the size of the radius of gyration, from 10^{-15} s for the bond vibration to 10^0 s for the chain diffusion.[1] On different scales, there are a series of well-developed simulation techniques, such as molecular dynamics (MD) and Monte-Carlo (MC) on the microscopic scale,[2,3] and dissipative particle dynamics (DPD),[4–6] lattice Boltzmann method (LBM),[7] dynamic density functional theory (DDFT),[8,9] and field-theoretic polymer simulation (FTPS)[10] on the mesoscale. These simulation methods are all focused on a specific scale, therefore it is urgent to build up a multiscale simulation method that can simulate on a larger time and length scale and keep enough microscopic information simultaneously.

Many researchers have worked hard in this field and come up with some constructive schemes from different points of view.[11–15] Some of these methods are based on fitting the radial distribution function (RDF), which links the micro- and mesoscale simulations by comparing coarse-grained RDF derived from atomistic simulations with the one from mesoscale simulations, then the potential of the mesoscale model is revised iteratively. After a few iterations, the RDF derived from mesoscale simulations is consistent with the target RDF and the updated potential between the coarse-grained beads is obtained. This potential can then be used to simulate a larger system under the same thermodynamic conditions. Representatives are the simplex algorithm (SA),[16–18] the iterative Boltzmann inversion (IBI)[19] method, and the reverse Monte-Carlo (RMC).[20–22] Some of the methods simulate coarse-grained systems in DPD framework with potentials derived from RMC[23]

or directly from mean field theory.[24] Some use DPD as a mesoscale simulation tool with interaction parameters fitted from isothermal compressibility[25] or from interfacial tension.[26] Also there are some algorithms which combine different length scales by simulating the fine-grained (FG) and the coarse-grained (CG) particles in one system.[27,28]

Stimulated by these pioneer works, we try to construct a coarse-grained model for polyethylene, which may be the most important polymeric material in industry, by mapping the RDF of the coarse-grained PE bead from the Lowe–Andersen temperature-controlling method (LA)[29,30] onto the target one from detailed molecular dynamics simulation. LA is selected in this research because this method is fast, stable, and easy to tune for a better temperature control. In the first step by fitting the RDF, we obtain a modified numerical coarse-grained potential. This potential, substituting the analytical conservative potential used in LA, is updated iteratively until the two RDFs are consistent with each other within error. This numerical potential can be applied in larger systems and the properties of PE on the mesoscale can be obtained. Because the potentials are always coupled with one another, it is difficult to fit the RDFs when there are too many potentials to be operated in one system.[19] The advantage of the present coarse-graining scheme is that there are only two kinds of potentials to be fitted, i.e., the nonbonded conservative potential and the bonded spring potential in a polymer chain, so it is easier to implement. After simulating the mesoscale PE systems using LA with the numerical coarse-grained potential, we can further fill the beads with atomistic details, i.e., do a fine-graining. In this way one may fast equilibrate the system by mesoscale simulation and still keep its atomistic details in a fine-graining step. By fixing bond lengths and bond angles, the atoms are regrown according to a scheme similar to Rosenbluth sampling.[3] Because the system is already in equilibrium, only tens of picoseconds of

* To whom correspondence should be addressed. E-mail: luzhy@mail.jlu.edu.cn.

MD run is needed to alleviate the local tension arising from the chain regrowing procedure.

This paper is organized as follows. In section 2 we briefly introduce the LA method, the automatic program to derive the coarse-grained potential for PE, and a scheme to fill the atoms into the coarse-grained bead and regrow the chain. In section 3 we describe the details of our simulation procedure for PE. In section 4 the coarse-grained potentials are tested by simulating the miscibility of the blends of LLDPE/HDPE and by investigating the scaling behavior of PE in bulk. Finally in section 5 we discuss the merits and limitations of our multiscale simulation method.

2. Methods

2.1. Lowe−Andersen Temperature-Controlling Method. LA is an alternative for DPD. Originally it uses the same conservative potential as in DPD, but with a different thermostat technique. The thermostat formed by the dissipative and random forces in DPD is substituted by the revised Andersen thermostat[29,32] in LA, which conserves momentum. An advantage of this method over DPD is that it can easily produce a higher Schmidt number to meet the requirement of modeling most of the real polymeric fluids. It shows excellent temperature control, gives correct radial distribution function, and works efficiently. With LA, it is possible to reproduce all the block copolymer microphase separation results as those obtained by conventional DPD simulations.[30] However, we adopt LA in this research mainly because LA can control the temperature very well. This feature is very important in the numerical potential fitting because it is harder to control the temperature when a numerical potential is applied, which is not as smooth as the analytical one.

The typical conservative force $\vec{F}_{ij}^C$ appearing in LA is a soft repulsion acting along the line of bead centers. With the velocity−Verlet algorithm we can first integrate Newton's equations of motion. Then for each pair of beads, we generate a relative velocity $\vec{v}_{ij}^o \cdot \hat{r}_{ij}$ from a Maxwell distribution $\xi_{ij}\sqrt{2k_BT^*/m}$, where $\hat{r}_{ij}$ indicates the velocity component parallel to the line of bead centers, and ξ_{ij} is a Gaussian distributed random number. To conserve momentum, we set $\vec{v}_i = \vec{v}_i + \vec{\Delta}_{ij}$, and $\vec{v}_j = \vec{v}_j - \vec{\Delta}_{ij}$, where $2\vec{\Delta}_{ij} = \hat{r}_{ij}(\vec{v}_{ij}^o - \vec{v}_{ij}) \cdot \hat{r}_{ij}$. Like DPD, only relative velocities are involved in the thermostat integration procedure, so the method is similarly Galilean invariant. The detailed LA scheme is listed in Table 1. When the simulated system contains chains, there is also a spring force between consecutive beads of the polymer: $\vec{F}_{ij}^b = C\vec{r}_{ij}$, with C being the spring constant.

2.2. Coarse-Graining Method. In a system of near zero density, the potential is approximately equal to the free energy,

$$F(r) = -k_BT \ln g(r) \tag{1}$$

SA, IBI, and RMC all take $F(r)$ as the first trial potential in the configuration simulation. $g(r)$, the radial distribution function, can be derived from MD or from experiments. The potentials needed to be modified always include the intramolecular potentials, such as the valence angle bending potential $V_{\text{angle}}(\theta)$ and the dihedral angle torsion potential $V_{\text{torsion}}(\phi)$, and the intermolecular potentials, such as the Lennard-Jones potential. The equation for updating the potentials used in SA and IBI is the same:

$$\phi_{i+1}(r) = \phi_i(r) + k_BT \ln\left(\frac{g_i(r)}{g(r)}\right) \tag{2}$$

TABLE 1: LA Approach

(1) $\vec{v}_i \leftarrow \vec{v}_i + \dfrac{1}{2}\dfrac{1}{m}\vec{F}_i^C \Delta t$

(2) $\vec{r}_i \leftarrow \vec{r}_i + \vec{v}_i \Delta t$

(3) calculate $\vec{F}_i^C\{\vec{r}_j\}$

(4) $\vec{v}_i \leftarrow \vec{v}_i + \dfrac{1}{2}\dfrac{1}{m}\vec{F}_i^C \Delta t$

(5) for all pairs of particles for which $r_{ij} < r_c$

   (i) generate $\vec{v}_{ij}^o \cdot \hat{r}_{ij}$ from a Maxwell distribution $\xi_{ij}\sqrt{2k_BT^*/m}$

   (ii) $2\vec{\Delta}_{ij} = \hat{r}_{ij}(\vec{v}_{ij}^o - \vec{v}_{ij}) \cdot \hat{r}_{ij}$

   (iii) $\vec{v}_i \leftarrow \vec{v}_i + \vec{\Delta}_{ij}$

   (iv) $\vec{v}_j \leftarrow \vec{v}_j - \vec{\Delta}_{ij}$

   with probability $\Gamma\Delta t$

Convergence can be measured quantitatively by evaluating the following merit function,

$$f_{\text{target}} = \int w(r)\,(g(r) - g_j(r))^2\,dr \tag{3}$$

where $w(r) = \exp(-r/\sigma)$ is a weighting function to penalize more strongly deviations at small distances. MD or MC is always used in the coarse-grained simulations in SA and IBI.

In RMC the trial potentials are updated iteratively according to

$$\phi_{\text{new}}(r) = \phi_{\text{old}}(r) + fk_BT \ln[g(r)_{\text{trial}}/g(r)_{\text{target}}] \tag{4}$$

where f is a constant used to obtain stable convergence of the potentials, and MC is used in the coarse-graining simulations.[22,31]

We update the coarse-grained potentials according to eq 4 as in RMC, while the trial RDF is produced through LA simulation by appropriately choosing the trial potential. In this framework, the potential and the RDF curves tend to fit well to the curves from MD in several iterations. Specifically, an updated numerical potential is produced with eq 4 and then replaces the old one in LA to start a new simulation. After a few iterations, $g(r)_{\text{trial}}$ is convergent to $g(r)_{\text{target}}$ which is obtained from MD. The procedure runs automatically until the difference between $g(r)_{\text{trial}}$ and $g(r)_{\text{target}}$ is within a designated small value. Finally the coarse-grained numerical potential is obtained.

2.3. Fine-Graining Method. To fill the atoms into the coarse-grained beads after equilibrium, first we randomly generate the coordinate of the first united atom (x_1, y_1, z_1) in one specific bead. With fixed bond length and bond angle, the second and third united atoms are also generated randomly. Then the ith ($i \geq 4$) united atom is generated following the Rosenbluth rule,[3] produce k random orientations from the $(i - 1)$th atom and calculate the energy $u_i(j)$ and the corresponding Boltzmann factor $w_i(j)$. Select an orientation n from the k orientations with a probability:

$$p_i(n) = \frac{\exp[-\beta u_i(n)]}{w_i(n)} \tag{5}$$

where $w_i(n)$ is defined as

$$w_i(n) = \sum_{j=1}^{k} \exp[-\beta u_i(j)]$$

Thus an atomistic detailed polymer chain can be produced atom after atom. An illustration of the chain growth is shown in Figure 1.
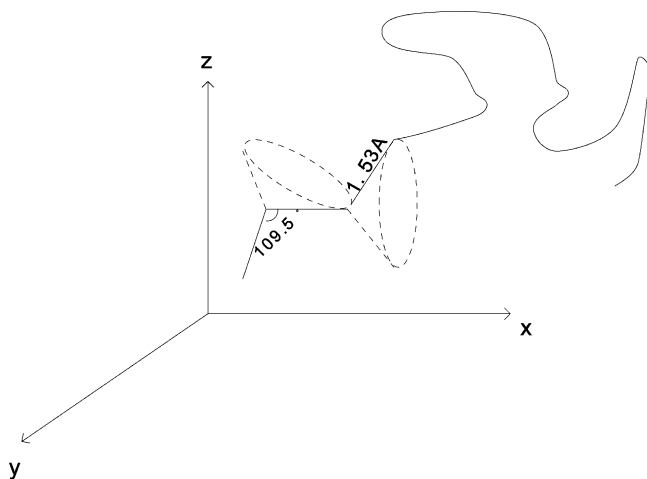
Coarse- and Fine-Graining Simulation of Polyethylene

J. Phys. Chem. B, Vol. 110, No. 47, 2006 **24095**

Figure 1. Illustration of chain growing. Bond length and angle are set to be 1.53 Å and 109.5°, respectively. The position of a new carbon is selected from 20 trial orientations depending on their Rosenbluth factors.
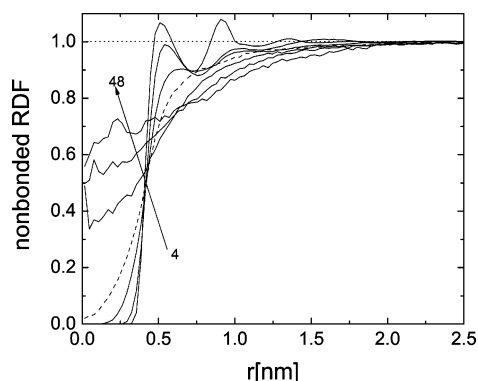

Figure 2. Nonbonded RDF calculated from MD simulations of C96 melts at 450 K with various coarse-graining levels λ = 4, 8, 12, 16, 24, 32, and 48.

3. Simulation Details

3.1. MD Simulation. MD simulations are performed for PE with chain length of 96 (denoted by C96) and 960 (C960) at 450 K in the NVT ensemble, respectively. The Dreiding force field[33] is applied to model the united atoms. However, as we have tested, using the parameters of the Dreiding force field, PE tends to form a crystal-like conformation at 450 K in NVT simulations with experimental density, and we cannot reproduce the correct density in NPT simulations. Therefore we re-fit the Lennard-Jones parameter ϵ for the atom type C_32 to obtain the experimental density of PE (766 kg/m^3) at 450 K[34] and find $\epsilon_{C\_32} = 0.08$ kcal/mol. Other parameters are kept unchanged. This modified Dreiding force field is then used in the NVT simulations of C96 and C960 systems, which contain 80 and 8 chains, respectively, giving the lengths of the boxes 61.611 and 61.583 Å. A time step of 2 fs is used. Equilibration runs of 1 ns are followed by 3 ns of production runs, and the configurations are saved every picosecond during the production run.

λ consecutive united atoms are then represented by a coarse-grained bead, which is located at the center of mass of that λ united atoms. The coarse-grained RDFs with various coarse-graining levels, i.e., λ = 4, 8, 12, 16, 24, 32, and 48, are calculated and shown in Figure 2. The curves show the same trends as in ref 22 for $\lambda \geq 8$. As can be seen in Figure 2, for λ = 4, 8, and 12, the beads exhibit a strong excluded volume effect. Therefore, the associated potential between coarse-grained beads at a short distance will show a strong repulsion

at these small λ values and is not "soft" enough. While for λ = 24, 32, and 48, the molecular details are apparently lost too much, when λ = 16, the beads are just going to overlap with each other and the repulsion between the beads at a short distance is "soft" to allow for a larger time step in solving Newton's equations of motion in the mesoscale simulations. Thus λ = 16 is an ideal candidate to balance between the computational efficiency and molecular details. In the next section we introduce the details on deriving the numerical coarse-grained potentials with λ = 16 for the C96 and C960 systems.

3.2. Obtaining Coarse-Grained Potentials. The thermodynamic state (e.g., the density and the temperature) of the MD systems and the mesoscopic LA systems must be kept the same. At the coarse-graining level λ = 16, the C96 chain corresponds to the 6-bead and the C960 chain corresponds to the 60-bead chain in the mesoscopic LA simulation, respectively. There is almost no correlation when the bead distance is larger than 12.5 Å as shown in Figure 2 for λ = 16. Therefore 12.32 Å is set to be the cutoff distance of the conservative force and the unit length in LA. Selecting 12.32 Å instead of 12.5 Å makes the reduced MD dimensionless box length an integer, i.e., 61.611/12.32 ≈ 61.583/12.32 ≈ 5, which gives a coarse-grained bead number density of 3.84 (= 6 × 80/(5 × 5 × 5) = 60 × 8/(5 × 5 × 5)). In the mesoscale LA simulations, we have selected two model systems. One contains 640 6-bead chains corresponding to the C96 system, the other contains 64 60-bead chains corresponding to the C960 system. The size of the simulation box in LA is 10 × 10 × 10, thus both systems have a bead number density of 3.84, which is exactly the same as that of the MD systems. The cutoff distance of the conservative force in LA is R_c = 1, which equals 12.32 Å in real length units. $k_B T$ is set as the unit of energy in the LA simulations while T = 450 K.

Setting the initial repulsion parameter a = 5, the spring constant C = 2, the thermal bath collision frequency Γ = 50, and a time step δt = 0.02, the two LA systems are simulated and the first nonbonded and bonded trial RDFs can be obtained. According to the unique theorem introduced by Henderson[35] and Gray and Gubbins,[36] in many-particle systems where the interactions are strictly pairwise additive, the interactions between constituents determine uniquely the pair distribution function and vice versa. The nonbonded RDF determines the conservative potential

$$\phi_{ij}^C(r) = \begin{cases} (a_{ij}R_c/2)(1 - r/R_c)^2 & (r < R_c) \\ 0 & (r \geq R_c) \end{cases} \quad (6)$$

The bonded RDF determines the conservative potential and the spring potential

$$\phi_{ij}^b(r) = -\frac{C}{2}r^2 \quad (7)$$

The conservative and the spring potentials are updated iteratively according to:

$$\phi_{new}^C(r) = \phi_{old}^C(r) + f k_B T \ln[g(r)_{trial}/g(r)_{target}]_{nonbonded}$$

$$[\phi_{new}^C(r) + \phi_{new}^b(r)] = [\phi_{old}^C(r) + \phi_{old}^b(r)] + \\ f k_B T \ln[g(r)_{trial}/g(r)_{target}]_{bonded} \quad (8)$$

According to eq 8, with the nonbonded and the bonded RDFs and the analytical $\phi_{old}^C(r)$ and $\phi_{old}^b(r)$, we obtain the first
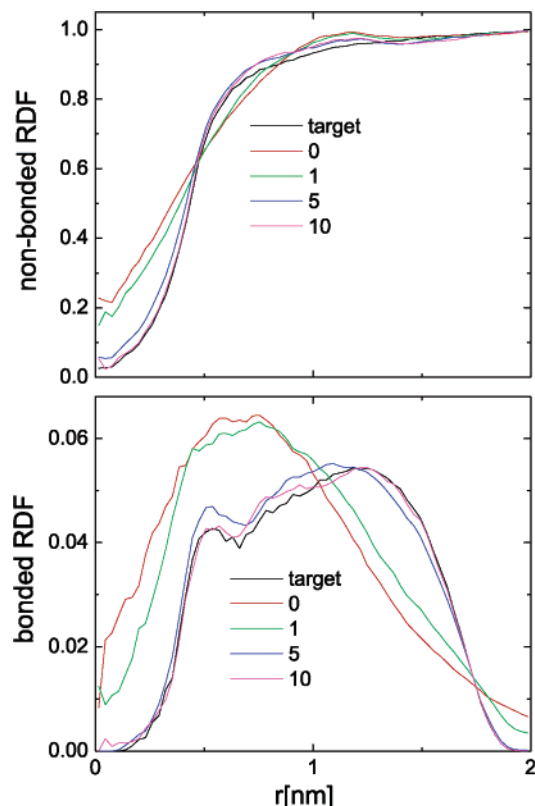
Figure 3. Fitting RDF to the target for the 60-bead per chain system in LA. In the figure, target denotes the target RDF, 0 the trial RDF produced by LA with the first trial analytical potential, and 1, 5, and 10 the RDF from the 1st, 5th, and 10th LA simulation iterations with the numerical potential.

Figure 4. Updating of the nonbonded and the bonded coarse-grained numerical potentials for the 60-bead per chain system with LA. The bonded potential includes conservative and spring potential between adjacent beads. 0 denotes the first trial analytical potential, and 1, 5, and 10 the numerical potentials for the 1st, 5th, and 10th iterations.

Figure 5. The RDFs and the corresponding fitted coarse-grained potentials for the C960 and the C96 systems. The nonbonded potentials are consistent with each other quite well, so the chain containing 96 carbons is long enough to derive coarse-grained potentials for PE. The potentials can be further used in larger systems of PE under the same thermodynamic conditions (for example, temperature and density).

numerical $\phi_{new}^{C}(r)$ and $\phi_{new}^{b}(r)$. The forces can be calculated via the interpolation algorithm[37] in the next LA simulation iteration. Thus after about 10 iterations, $g(r)_{trial}$ gradually converges to $g(r)_{target}$ and the effective numerical potentials are derived for PE at 450 K with the coarse-graining level $\lambda = 16$. Figure 3 shows some typical RDFs during the fitting iterations and Figure 4 shows the corresponding potentials for the system of 60-bead chains. We can see that it is impossible to fit the potentials in analytical forms.

The upper panel of Figure 5 shows the target nonbonded RDFs for the C960 and C96 systems, while the lower panel shows the corresponding fitted potentials. As can be seen in Figure 5, the nonbonded RDFs are almost the same for the two systems. The fitted nonbonded potentials of the C960 and C96 systems are almost equivalent with each other, their differences are not so pronounced to vary the physical properties of the two systems very much. Therefore, the coarse-grained potentials derived with chain length 96 are enough to represent the numerical coarse-grained potentials for longer PE chain under specific thermodynamics conditions ($T = 450$ K, $\rho = 766$ kg/m³, and $\lambda = 16$).

3.3. Fine-Graining of the Fully Equilibrated LA System. With the derived numerical coarse-grained potentials, the system containing 64 60-bead chains is simulated long enough with LA to be fully equilibrated. Atomistic details can then be filled into the coarse-grained beads. Setting the bond length to 1.53 Å and bond angle to 109.5°, we regrow the chains by filling every bead with 16 united carbon atoms using the method introduced in section 2.3. A 16-carbon alkane chain roughly has a radius of gyration $R_g \approx N^{1/2}b = 15^{1/2} \times 1.53 \approx 5.9$ Å, i.e., the average distance between the 16 carbons and the position of the bead mass center can be set as 5.9 Å. Practically in the
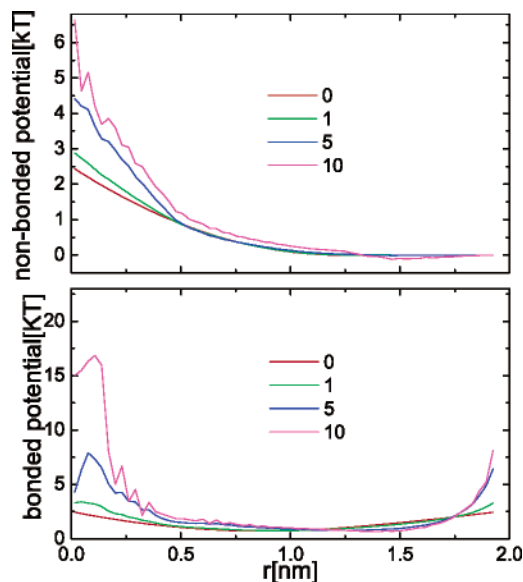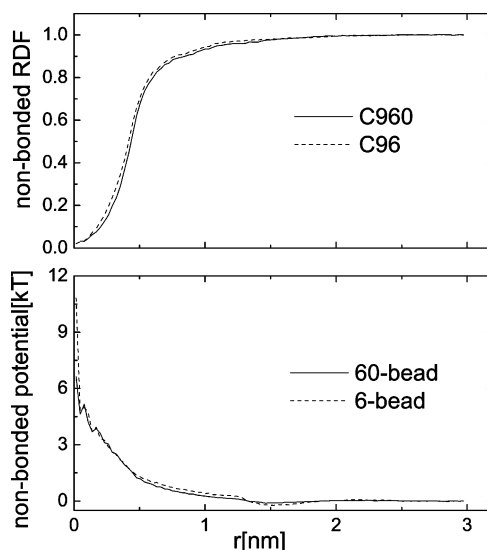
chain-growing process, the 16 carbons are generated no more than 8 Å away from the position of the bead mass center. Another restriction for this atom generation is that the distance between the center of mass of the generated 16 united carbons and the coarse-grained bead is no more than 1.5 Å. These two restrictions are actually selected for compromising between a correct configuration production and the computational efficiency. The first carbon atom in the following bead and the last carbon atom in the former bead are just connected together by a bond. So the bond lengths (for example, the bond between C16 and C17) and the bond angles (for example, the angle formed by C15, C16, and C17) around the joints are not the set values. Thus the united carbon atoms can be inserted bead by bead and chain after chain. Each united carbon atom to be grown
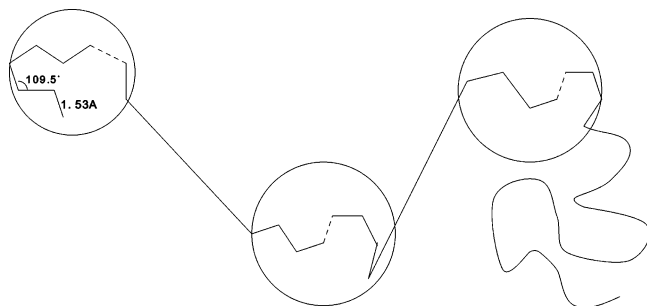
Coarse- and Fine-Graining Simulation of Polyethylene

J. Phys. Chem. B, Vol. 110, No. 47, 2006 **24097**

Figure 6. Illustration of bead-by-bead chain growing. Sixteen united carbon atoms are filled in each bead. The last atom in the former bead and the first atom in the following bead are just connected by a virtual bond. This unphysical bond construction will be relaxed and corrected in the following MD simulations.
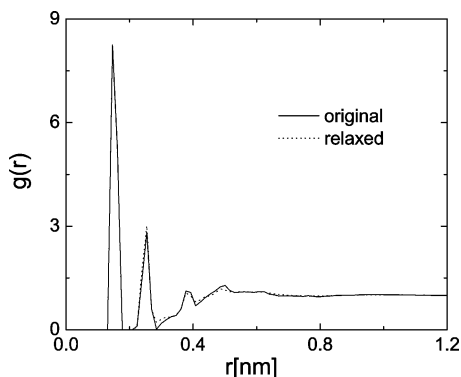

Figure 7. Comparison of the atomistic RDF obtained from original MD simulation and from fine-graining with relaxation. They are consistent with each other quite well, confirming the reliability of our fine-graining method.

is subjected to the Lennard-Jones potential, and its most suitable position is selected according to eq 5 to avoid strong overlapping. An illustration of this bead by bead regrowing procedure is shown in Figure 6.

The grown atomistic system possesses tension induced by those improper bond lengths and angles around bead joints and should be relaxed. We then run the atomistic MD a few picoseconds to relax the unphysical tension. It should be noted that in this step, the Lennard-Jones parameters for the united atoms are smoothly increased from very small values until they reach the correct values to avoid a drastic energy increase. Thus the microscopic configuration of a large polymeric system can be produced. In fact, it is still not easy to build up a reasonable microscopic configuration of large polymeric systems with long chains, especially in the glassy state.[38,39] The present scheme may be a promising alternative for this purpose by combining the coarse-graining and fine-graining together followed by a local minimization. Figure 7 shows the atomistic RDF obtained by fine-graining with relaxation and the original RDF from the atomistic detailed MD simulation for the C960 system. The atomistic RDFs agree with each other quite well, confirming the reliability of our fine-graining method.

It should be noted that the coarse-graining process leads to the reduction in degrees of freedom, and therefore, different entropy. The coarse-grained Hamiltonian is parametrized to describe the structural correlation correctly, but not the internal energy. Therefore, thermodynamic quantities such as pressure cannot be correctly reproduced for the coarse-grained system. However, this problem can be avoided if a successful fine-graining method is available.[22]
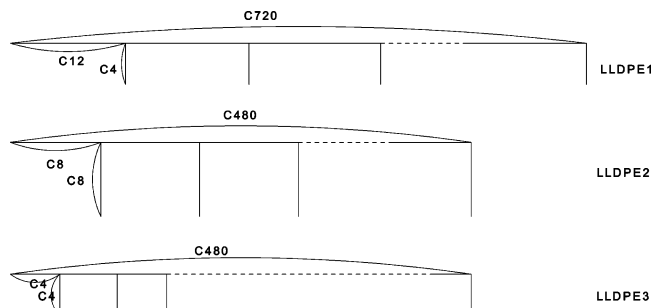

Figure 8. Illustration of the three LLDPE models: (1) LLDPE1, 60 4-carbon branches per 720 main chain carbons; (2) LLDPE2, 60 8-carbon branches per 480 main chain carbons; and (3) LLDPE3, 120 4-carbon branches per 480 long chain carbons.

4. Application of the Multiscale Simulation Method

4.1. Miscibility of HDPE and LLDPE. In industry, different types of PE are often blended together to meet various requirements of processing and result in a better quality of the final products, therefore the understanding of the phase behavior of PE blends is of great importance. It has been found that phase separation of linear low-density polyethylene (LLDPE)/high-density polyethylene (HDPE) blends occurs when the branch content of LLDPE molecules is above a certain value.[40]

In this research we have selected three model LLDPE molecules with different branch contents and studied their miscibility with HDPE, using the LA method with the numerical coarse-grained potentials. The HDPE is the C960 system, which is introduced in section 3.2. The three branched LLDPE models also contain 960 united carbon atoms and the branches all orderly branched on the main chain in all three models to simplify the model. The first model LLDPE system is 60 4-carbon branches attached on the main chain every 12 carbons (denoted by LLDPE1). The second model LLDPE system is 60 8-carbon branches attached on the main chain every 8 carbons (denoted by LLDPE2). The third model LLDPE system is 120 4-carbon branches attached on the main chain every 4 carbons (denoted by LLDPE3). The illustration of the three LLDPE models is shown in Figure 8. We obtain the effective coarse-grained potentials for the three branched LLDPE systems with the same coarse-graining procedure as used in the HDPE system. MD simulations are first run at 450 K with the modified Dreiding force field for the three LLDPE systems which contain 8 chains each, giving the box length 61.583 Å. The Lennard-Jones parameters ϵ for C_31 and C_32 are 0.06 and 0.08 kcal/mol, respectively, which are obtained by fitting the parameters so that the correct physical density is ensured in NPT simulations. As in the HDPE simulations, every 16 united carbon atoms (including the main chain atoms and the branch atoms) are grouped into one bead successively. It should be noted that a more precise scheme for grouping the monomers was put forward by Guerrault et al.[24] However, we have taken the simplest method in this research that is fast and easy to implement. Then 64 60-bead chains are put into a 10 × 10 × 10 box, which is simulated with LA. By fitting the calculated coarse-grained RDFs of the three LLDPE model systems in LA to those obtained in MD simulations according to eq 8, we can obtain, with several iterations, the coarse-grained numerical potentials of the three LLDPE models. These final RDFs and the potentials, together with those of the HDPE model, are shown in Figure 9 for a comparison. Apparently, the coarse-grained RDFs and the numerical potentials of the three LLDPE models are all quite different from those of the HDPE model, especially for LLDPE3.
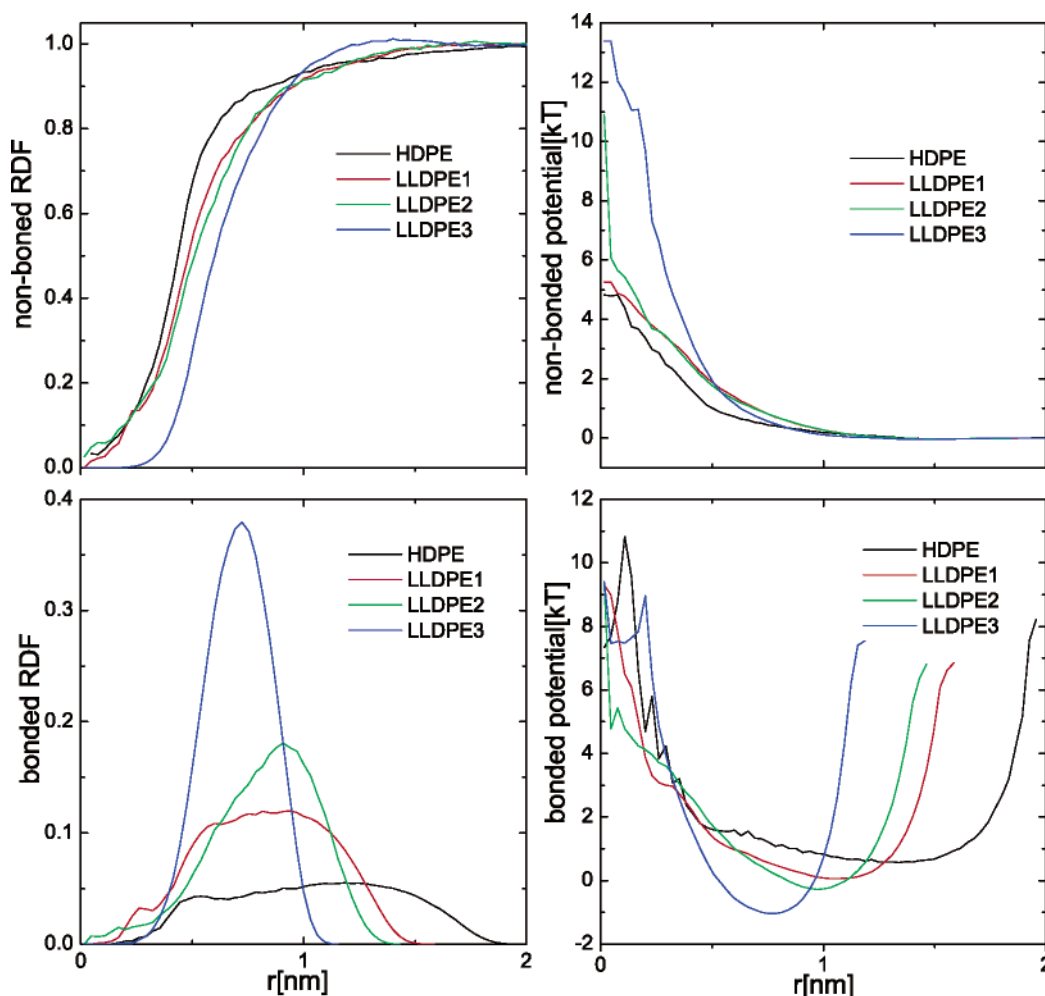
Figure 9. Coarse-grained RDFs and the corresponding numerical potentials for the three LLDPE and the HDPE models.

Three blend systems LLDPE1/HDPE, LLDPE2/HDPE, and LLDPE3/HDPE are simulated by using the LA method with the coarse-grained numerical potentials. The bath collision frequency Γ is taken to be 50 and the time step to be 0.02, the same as those in deriving the numerical potentials. The LLDPE and HDPE chains are mixed together with equal volume fraction, giving a total bead number density of 3.84. With the numerical potentials of LLDPE and HDPE models at 450 K, the forces between the same kind of beads are determined with the interpolating algorithm. The potential between different types of beads is calculated by the geometric combination rule:

$$\phi_{ij} = [\phi_{it}\phi_{jj}]^{1/2} \tag{9}$$

After about 6000 LA time units, separation occurs in the blend of LLDPE3/HDPE, indicated by a clear interface in the isodensity plot shown in Figure 10. The fluctuation of the interface may be due to the strong coupling of the thermostat (ΓΔt = 1). Phase separations of the blends LLDPE1/HDPE and LLDPE2/HDPE also take place but much more slowly (after about 10 000 LA time units). Their phase interfaces are somehow not so clear. The differences in the speed of phase separation and the shape of isodensity surface between the blend LLDPE1/HDPE and LLDPE2/HDPE are small. This is reasonable because the differences of the nonbonded RDFs and the potentials between the LLDPE1 and LLDPE2 model are small, as shown in Figure 9. The ambiguity of the phase interfaces of the two blend systems may be because the differences of the potentials between LLDPE1 (or LLDPE2) and HDPE are not
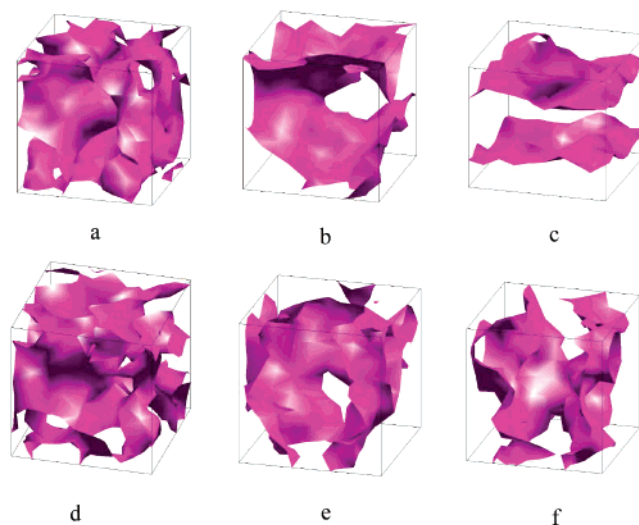

Figure 10. Time evolution of the isodensity surfaces of the LLDPE/HDPE blend systems. The upper three panels are for LLDPE3/HDPE after (a) 300, (b) 4000, and (c) 6000 time units. The lower three panels are for LLDPE1/HDPE after (d) 300, (e) 8000, and (f) 10000 time units.

remarkable and a high Γ value may slow the chain diffusion. As a comparison, the isodensity surface of blend LLDPE1/HDPE is also shown in Figure 10.

Our simulations reproduce phase separations of the LLDPE/HDPE blends, which shows that the coarse-grained potentials
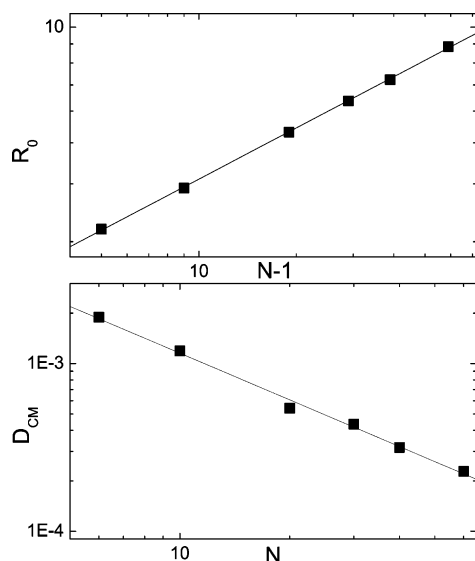
Coarse- and Fine-Graining Simulation of Polyethylene

J. Phys. Chem. B, Vol. 110, No. 47, 2006 **24099**

Figure 11. R_0 and D_{CM} as a function of the number of beads N for HDPE. The slopes of the linear fitted lines are 0.51 for R_0 and -0.95 for D_{CM}, respectively.

somehow contain sufficient information regarding local phase behavior. It is argued that entropy changes when coarse-graining is carried out, then the coarse-grained Hamiltonian, and therefore the phase behavior, is different from that of the underlying molecular systems.[22,41] In our method, the entropy difference between LLDPE and HDPE is implicitly embodied in the difference of the coarse-grained RDFs, and consequently transferred into the potential energy difference between LLDPE and HDPE, therefore the local phase separation can take place.

4.2. Scaling Law. The quantities measured in the LA simulations are the root-mean-squared end-to-end distance R_0 and the diffusion coefficient of the polymer center of mass D_{CM}. D_{CM} is calculated from the slope of the long time behavior of the mean-square displacement of the center of mass,

$$D_{CM} = \lim_{t \to \infty} \frac{1}{6t} \langle [\vec{R}_{CM}(t) - \vec{R}_{CM}(0)]^2 \rangle \qquad (10)$$

In LA simulations, Chen et al. showed that regardless the value of Γ, the polymers obey the Rouse scaling.[30] With the numerical coarse-grained potential obtained above for HDPE, R_0 and D_{CM} are calculated for different chain lengths using the LA method. The Rouse scalings $R_0 \approx (N-1)^{1/2}$ and $D_{CM} \approx N^{-1}$ observed by Spenley in DPD simulations[42] are recovered in the present study, which are illustrated in Figure 11. Like the original analytical conservative potential, the coarse-grained numerical potential is also soft. Thus the force between two beads is always finite so that the beads can overlap and even go through each other easily. This unphysical chain behavior is inherent in lots of soft potential simulation techniques, which benefits fast equilibrium and a larger time step. However, it also limits the application of these simulation methods, which is only valid before reptation and chain entanglements set in. We note that by carefully selecting the integration time step and increasing the bead repulsions in DPD, it is possible to study the reptation behavior of polymer melts.[43]

5. Conclusions

We have suggested an automatic coarse-graining method and derived the coarse-grained numerical potential for PE. Moreover we have introduced a possible scheme, based on the Rosenbluth sampling, to fine-grain the large equilibrated coarse-grained

system that may be further used in MD simulations. By doing this we can benefit from accessing the equilibrium fast enough on a mesoscopic time and length scale.

During the coarse-graining, two HDPE models (C960 and C96) are simulated with MD to obtain the target coarse-grained RDFs, which are then compared with the RDFs from LA simulations to derive the coarse-grained numerical potentials at the specific thermodynamic conditions iteratively. With the coarse-grained numerical potential, we test the scaling behavior of the model HDPE and find that it obeys the Rouse scaling with $R_0 \approx N^{1/2}$ and $D_{CM} \approx N^{-1}$. This is in agreement with the results of refs 30 and 42, implying that our coarse-graining method is correct. To further test the validity of the method on deriving the coarse-grained numerical potential, at 450 K, three model PE blend systems are simulated with LA to study the miscibility of the blends. The coarse-grained potentials for LLDPE are derived by using the same method as in deriving the potential for HDPE, though with the simple coarse-graining scheme, phase segregation does occur for all three systems with the branch content of LLDPE well above the critical value suggested by Choi. This qualitatively verifies the correctness of our coarse-grained numerical potential and confirms the feasibility of our coarse-graining methodology. Fine-graining of the large systems which have been equilibrated with LA adopting the coarse-grained numerical potentials is also tested with a growing-chain program followed by a relaxing procedure. The difference between the original RDF from MD simulation and the one from fine-graining after relaxation is rather small, which confirms the validity of our method. The obtained large atomistic system may be used for further study such as investigating the mechanical properties. Building more representative coarse-grained models for LLDPE and further improving our fine-graining scheme are the issues of our future study.

References and Notes

(1) Müller-Plathe, F. *ChemPhysChem* **2002**, *3*, 754.

(2) Allen, M. P.; Tildesley, D. J. *Computer Simulation of Liquids*; Clarendon: Oxford, UK, 1987.

(3) Frenkel, D.; Smit, B. *Understanding Molecular Simulation*: *From Algorithms to Applications*; Academic Press: San Diego, CA, 1996.

(4) Hoogerbrugge, P. J.; Koelman, J. M. V. A. *Europhys. Lett.* **1992**, *19*, 155.

(5) Español, P.; Warren, P. B. *Europhys. Lett.* **1995**, *30*, 191.

(6) Groot, R. D.; Warren P. B. *J. Chem. Phys.* **1997**, *107*, 4423.

(7) Chen, S.; Doolen, G. D. *Annu. Rev. Fluid Mech.* **2001**, *30*, 329.

(8) Fraaije, J. G. E. M.; van Vlimmeren, B. A. C.; Maurits, N. M.; Postma, M.; Evers, O. A.; Hoffman, C.; Altevogt, P.; Goldbeck-Wood, G. *J. Chem. Phys.* **1997**, *106*, 4260.

(9) van Vlimmeren, B. A. C.; Maurits, N. M.; Zvelindovsky, A. V.; Sevink, G. J. A.; Fraaije, J. G. E. M. *Macromolecules* **1999**, *32*, 646.

(10) Fredrickson, G. H.; Ganesan, V.; Drolet, F. *Macromolecules* **2002**, *35*, 16.

(11) Tschop, W.; Kremer, K.; Batoulis, J.; Burger, T.; Hahn, O. *Acta Polym.* **1998**, *49*, 61.

(12) Tschop, W.; Kremer, K.; Batoulis, J.; Burger, T.; Hahn, O. *Acta Polym.* **1998**, *49*, 75.

(13) Izvekov, S.; Voth, G. A. *J. Phys. Chem. B* **2005**, *109*, 2469.

(14) Izvekov, S.; Violi, A.; Voth, G. A. *J. Phys. Chem. B* **2005**, *109*, 17019.

(15) Queyroy, S.; Neyertz, S.; Brown, D.; Müller-Plathe, F. *Macromolecules* **2004**, *37*, 7338.

(16) Faller, R.; Schmitz, H.; Biermann, O.; Müller-Plathe, F. *J. Comput. Chem.* **1999**, *20*, 1009.

(17) Meyer, H.; Biermann, O.; Faller, R.; Reith, D.; Müller-Plathe, F. *J. Chem. Phys.* **2000**, *113*, 6264.

(18) Reith, D.; Meyer, H.; Müller-Plathe, F. *Macromolecules* **2001**, *34*, 2335.

(19) Reith, D.; Pütz, M.; Müller-Plathe, F. *J. Comput. Chem.* **2003**, *24*, 1624.

(20) Lyubartsev, A. P.; Laaksonen, A. *Phys. Rev. E* **1995**, *52*, 3730.

(21) Soper, A. K. *Chem. Phys.* **1996**, *202*, 295.

(22) Ashbaugh, H. S.; Patel, H. A.; Kumar, S. K.; Garde, S. *J. Chem. Phys.* **2005**, *122*, 104908.

(23) Lyubartsev, A. P.; Karttunen, M.; Vattulainen, I.; Laaksonen, A. *Soft Mater.* **2003**, *1*, 121.

(24) Guerrault, X.; Rousseau, B.; Farago, J. *J. Chem. Phys.* **2004**, *121*, 6538.

(25) Groot, R. D.; Rabone, K. L. *Biophys. J.* **2001**, *81*, 725.

(26) Maiti, A.; McGrother, S. *J. Chem. Phys.* **2004**, *120*, 1594.

(27) Backer, J. A.; Lowe, C. P.; Hoefsloot, H. C. J.; Iedema, P. D. *J. Chem. Phys.* **2005**, *123*, 114905.

(28) Christen, M.; van Gunsteren, W. F. *J. Chem. Phys.* **2006**, *124*, 154106.

(29) Lowe, C. P. *Europhys. Lett.* **1999**, *47*, 145.

(30) Chen, L. J.; Lu, Z. Y.; Qian, H. J.; Li, Z. S.; Sun, C. C. *J. Chem. Phys.* **2005**, *122*, 104709.

(31) Garde, S.; Ashbaugh, H. S. *J. Chem. Phys.* **2001**, *115*, 977.

(32) Andersen, H. C. *J. Chem. Phys.* **1980**, *72*, 2384.

(33) Mayo, S. L.; Olafson, B. D.; Goddard, W. A., III *J. Phys. Chem.* **1990**, *94*, 8897.

(34) Paul, D. R.; Di Benedetto, A. T. *J. Polym. Sci.*, *Part C*: *Polym. Symp.* **1965**, *10*, 17.

(35) Henderson, R. L. *Phys. Lett.* **1974**, *49A*, 197.

(36) Gray, C. G.; Gubbins, K. E. *Theory of Molecular Fluids*: *Fundamentals*: Clarendon: Oxford, UK, 1984; Vol. 1, p 178.

(37) Press, W. H.; Teukolsky, S. A.; Vetterling, W. T.; Flannery, B. P. *Numerical Recipes in C*: *The Art of Scientific Computing*: Cambridge University: Cambridge, UK, 1988.

(38) Kotelyanskii, M.; Wagner, N. J.; Paulaitis, M. E. *Macromolecules* **1996**, *29*, 8497.

(39) Müller, M.; Nievergelt, J.; Santos, S.; Suter, U. W. *J. Chem. Phys.* **2001**, *114*, 9764.

(40) Choi, P. *Polymer* **2000**, *41*, 8741.

(41) Jain, S.; Garde, S.; Kumar, S. K. *Ind. Eng. Chem. Res.* **2006**, *45*, 5614.

(42) Spenley, N. A. *Europhys. Lett.* **2000**, *49*, 534.

(43) Nikunen, P.; Vattulainen, I.; Karttunen, M. Arxiv: cond-mat/0512248.